DOI: 10.31276/VJSTE.65(2).03-09

Density functional theory studies on molecular structure, vibrational spectra, AIM, HOMO-LUMO, electronic properties, and NBO analysis of benzoic acid monomer and dimer

Tan Trung Truong[1*], Phuong Dong Nguyen[2], Thi Ngan Nguyen[1], Thi Thu Thuy Le[1], Ngoc Huong Nguyen[1]

[1]Dong Nai Technology University, 5 Nguyen Khuyen Street, Trang Dai Ward, Bien Hoa City, Dong Nai Province, Vietnam
[2]Department of Chemistry, Soongsil University, 369 Sangdo-ro, Dongjak-gu, Seoul, Korea

Received 14 January 2022 ; accepted 29 March 2022

Abstract:

In this study, the molecular structure, vibrational frequencies, and atom-in-molecule (AIM) analysis of the benzoic acid monomer and dimer were investigated. Geometry optimization and vibrational frequency calculations for the monomer and dimer were carried out at the density functional theory (DFT) level with the 6-311++G(2d,p) basis set. UV-Vis spectroscopy and electronic properties (i.e., excitation energies, oscillator strengths) were calculated by time-dependent DFT (TD-DFT) in different solvents. The calculated absorption values mainly represented excitation from HOMO-1 (H-1) → LUMO and HOMO → LUMO+2 (L+2). The structure-activity relationship was interpreted by its molecular electrostatic potential (MEP) surface, which is very useful to the research of molecular structures and their physiochemical-property relationships. The highest occupied molecular orbital (HOMO)-lowest unoccupied molecular orbital (LUMO) energy was analysed. The HOMO-LUMO energy gap and other related molecular properties were also calculated. In addition, natural bond orbital (NBO) analysis was carried out to investigate the various intra-intermolecular interactions in the molecular system.

Keywords: **atom-in-molecule, benzoic acid, highest occupied molecular orbital-lowest unoccupied molecular orbital analysis, molecular electrostatic potential, natural bond orbital.**

Classification numbers: **2.1, 2.2**

1. Introduction

Benzoic acid is chemically known as benzene carboxylic acid. Its molecular formula is C_6H_5COOH. This colourless crystalline solid is the simplest aromatic carboxylic acid, which has been known for a long time as the source of a large number of synthesis processes of organic compounds. Indeed, many organic compounds have been synthesized from benzoic acid in many industries and its use in the production of glycol benzoates as plasticizers in adhesive formulations is increasing [1]. Besides, salts and esters of benzoic acid are used as preservatives in foods, drugs, and personal products. In the treatment of fungal skin disease and other diseases such as tines, ringworm, and athlete's foot, benzoic acid is the vital component of benzoin resins and ointments [2].

Hydrogen bonded (A−H···B) molecules have been considered as major points of interest due to their very important role in many fields like chemistry, physics, and biology [3]. Crystal structures of benzoic acids have been determined from neutron diffraction over temperatures between 20-175 K [4]. Molecules can form cyclic hydrogen bond dimers between the carboxylic acid group. In recent years, infrared spectra of the OH stretch region of benzoic acid dimers has been studied by G.M. Florio, et al. (2001) [5] using the double resonance method of fluorescence-dip IR spectroscopy in a supersonic jet. The authors have also computed theoretical IR spectra of the benzoic acid dimer [5, 6]. The infrared spectrum of hydrogen-bonded benzoic acid has been recorded previously [7] and more recently by M. Boczar, et al. (2004) [8]. The geometric structures of the benzoic acid molecule have been investigated by A. Kumer, et al. (2019) [9]. The optimized structural parameters and HOMO, LUMO of the benzoic acid molecule are provided from theoretical calculations using HyperChem 8.0.10 software, but the effect of hydrogen bonding, charge transfer, and NBO analysis has not yet been discussed.

To the best of our knowledge, an extensive investigation of the structural, vibrational, and electronic properties of the monomer and dimer of benzoic acid have not been reported yet in the literature. Hence, we focused our investigation on the monomer and dimer of benzoic acid in the gas phase as we are interested in the dominant contribution to intermolecular interaction between two monomers. The

*Corresponding author: Email: truongtantrung@dntu.edu.vn

detail of vibrational infrared and UV-Vis spectra of benzoic acid molecules were analysed by computational results. Besides, the energy values of HOMO and LUMO molecular orbitals with their corresponding HOMO-LUMO energy gap are studied. In addition, the stabilization resonance energy $E^{(2)}$ was calculated by NBO analysis. Finally, the structure-chemical reactivity relationship and the MEP surface of the title compound were undertaken for the first time.

2. Computational methods

The molecular structure of the title compound was fully optimized at the DFT level using the hybrid functional B3LYP (Becke's three-parameter exchange functional [10] combined with the Lee-Yang-Parr correlation functional [11]) with the 6-311++G(2d,p) basis set [12]. Topological parameters such as electron density (ρ(r)), Laplacian of electron density (∇^2(ρ®), electron kinetic energy density (G(r)), and electron potential energy density (V(r)) at bond critical points (BCP) of intermolecular interactions were identified using AIM 2000 [13] software based on Bader's atom in molecules theory. NBO calculations were performed using GenNBO 5.G [14] as implemented in the Gaussian 09 package at the DFT/B3LYP/6-311++G(2d,p) level. Besides, the MEP [15] of benzoic acid was investigated using theoretical calculations. All calculations were carried out using the GAUSSIAN 09 program [16]. The GaussView program [17] was considered to obtain visual animations and also for the verification of the normal modes assignment.

3. Results and discussion

3.1. Molecular geometry

The optimized geometrical structure of the title compound dimer was performed in the gas phase by DFT at the B3LYP/6-311++G(2d,p) basis set and is presented in Fig. 1. The selected geometric parameters are tabulated in Table 1.

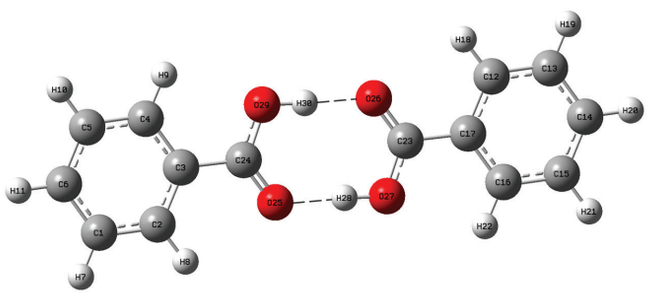

Fig. 1. The optimized geometric structure of benzoic acid dimer by B3LYP/6-311++G(2d,p).

The molecular structure of the benzoic acid dimer is formed by two benzoic acid monomers. The intermolecular hydrogen bond distances are shown in Table 1. The strong intermolecular interaction O27–H28···O25 is formed with a bond distance of 1.637 Å. At the B3LYP/6-311++G** and B3LYP/cc-pVTZ levels, the lengths of O–H···O were 1.663 Å and 1.635 Å, respectively [8], while the distance between O26(27)···O29(25) is about 2.641 Å. The difference between the calculated value in this work and in the literature [8] is around 0.022 Å. As can be seen in Table 1, most of the bond lengths and bond angles estimated at the B3LYP/6-311++G(2d,p) level agree with experimental values.

Table 1. Selected parameters of an optimized geometric of benzoic acid dimer by B3LYP/6-311++G(2d,p).

Parameters	B3LYP/6-311++G(2d,p)	Experimental
Bond lengths (Å)		
C24–O29	1.319	1.29[b]
C24–O25	1.230	1.24[b]
C24–C3	1.485	1.48[b]
C1–C2	1.388	1.42[b]
C2–C3	1.397	1.39[b]
C3–C4	1.397	1.39[b]
C4–C5	1.389	1.41[b]
C5–C6	1.392	1.36[b]
C1–H7	1.083	0.96[b]
C2–H8	1.082	0.79[b]
C4–H9	1.081	0.79[b]
C5–H10	1.083	0.96[b]
C6–H11	1.084	0.91[b]
Bond angles (°)		
O25–C24–O29	123.319	122[b]
C3–C24–O29	114.663	118[b]
C3–C24–O25	122.018	122[b]
Intermolecular H-bond lengths (Å) and angles (°)		
C23–O26–H30	124.88	
CH23–O27–H28	110.41	
O26(27)···O29(25)	2.641	2.64[a]; 2.629[b]
O27–H28···O25	1.637	1.64[b]

Note: [a]: Ref. [18]; [b]: Ref. [19].

In addition, the thermodynamic properties (i.e., zero-point vibrational energy, electronic energy, entropy, enthalpy, and free energy) of a benzoic acid molecule in the gas phase and in a solvent phase (water, methanol, and ethanol) are presented in Table 2. It can be clearly observed from Table 2 that the effects of the solvent phase can be seen in the thermodynamic properties and electronic energy (E) of the solvents, which decrease in the order of gas > water > methanol > ethanol. This shows that molecules of benzoic acid become stabilized in less polar solvents.

Table 2. Calculated thermodynamic properties for benzoic acid with DFT/B3LYP/6-311G++(2d,p).

Phase	ZPVE[a]	E[b]	S[c]	H[d]	F[e]
Gas	72.2014	-264151.7618	84.6390	77.2835	52.0486
Water	71.8701	-264157.6992	85.2760	76.9811	51.5567
Methanol	71.9366	-264159.9909	85.1460	77.0382	51.6520
Ethanol	71.9535	-264160.3021	85.1610	77.0507	51.6602

Note: [a]: Zero-point vibrational energy (ZPVE) (kcal/mol); [b]: Electronic energy (E) (kcal/mol); [c]: Entropy (S) (cal/mol-K); [d]: Enthalpy (H) (kcal/mol); [e]: Free energy (F) (kcal/mol).

3.2. UV-Vis and electronic properties

The solvents' effect on UV-Vis spectra and electronic properties were calculated with DFT based on the CAM-B3LYP [20] using different levels of theory. Theoretical optical absorption spectrum for the gas phase and solvents such as water, methanol (MeOH), and ethanol (EtOH) of benzoic acid in the wavelength region of 150-300 nm is displayed in Fig. 2. The calculated absorption wavelength, excitation energies, and oscillator strengths of benzoic acid were gathered in Table 3.

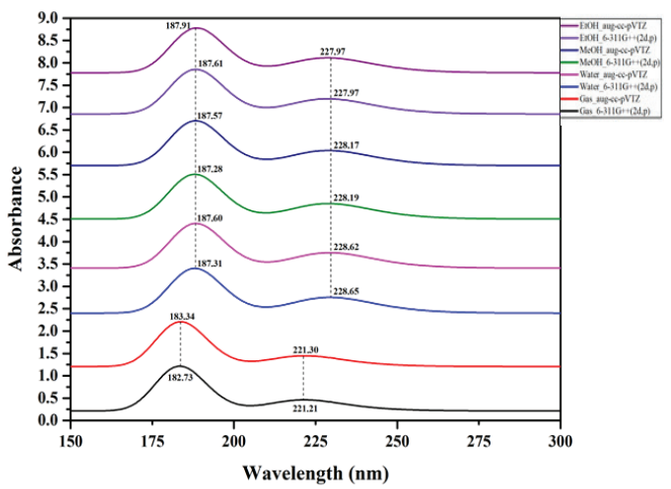

Fig. 2. UV-Vis absorption spectra of benzoic acid in gas phase and in various solvents at different levels of theory.

As it can be seen in Fig. 2 and Table 3, the calculated absorption value for benzoic acid in gas phase have been found to be 183 nm (excited state 5) and 221 nm (excited state 3). This peak mainly represents excitation from HOMO-1 (H-1) → LUMO (73%) and HOMO → LUMO+2 (L+2) (75%). In water, the ~188-nm peak (excited state 5) and ~229-nm peak (excited state 3) for benzoic acid were predicted by DFT. Its major contributions were (H-1) → LUMO (90%) and HOMO → (L+2) (89%). The ~188-nm peak (6.52-6.54 eV) and ~228-nm peak (5.43-5.44 eV) were predicted in MeOH and EtOH solvents by DFT/CAM-B3LYP with 6-311G++(2d,p) and aug-cc-pVTZ basis sets, respectively. The major contributions were (H-1) → LUMO (90%) and HOMO → (L+2) (88%) for MeOH solvent and (H-1) → LUMO (89%) and HOMO → (L+2) (88%) for EtOH solvent.

Table 3. The calculated absorption wavelength λ (nm), excitation energy E (eV), and oscillator strength (f) of benzoic acid in gas phase and various solvents (water, MeOH, EtOH).

Solvent	State	TD-DFT/CAM-B3LYP/6-311G++(2d,p)				TD-DFT/CAM-B3LYP/aug-cc-pVTZ			
		λ (nm)	*E (eV)*	*Osc. Strength*	*MO contribution*	*λ (nm)*	*E (eV)*	*Osc. Strength*	*MO contribution*
Gas	1	242.43	5.11	0.0202		242.29	5.12	0.0196	
	2	237.67	5.22	0.0000		238.70	5.19	0.0000	
	3	221.21	5.60	0.2136	From H-1 to LUMO (73%), from HOMO to LUMO (14%), from HOMO to L+2 (10%)	221.30	5.60	0.2105	From H-1 to LUMO (72%), from HOMO to LUMO (15%), from HOMO to L+3 (10%)
	4	185.26	6.69	0.2683		185.59	6.68	0.2653	
	5	182.73	6.79	0.6232	From H-1 to LUMO (10%), from HOMO to L+2 (75%), from H-1 to L+2 (8%), from H-1 to L+10 (2%)	183.34	6.76	0.0008	From HOMO to L+1 (80%), from H-1 to L+1 (3%), from HOMO to L+2 (4%), HOMO to L+5 (3%), HOMO to L+15 (4%)
	6	182.42	6.80	0.0007		182.99	6.78	0.6311	
	7	180.16	6.88	0.0068		181.13	6.84	0.0063	
	8	171.08	7.25	0.0000		172.20	7.20	0.0000	
Water	1	247.14	5.02	0.0373		246.99	5.02	0.0365	
	2	230.54	5.38	0.0000		231.11	5.36	0.0000	
	3	228.65	5.42	0.3252	From H-1 to LUMO (90%), from HOMO to L+2 (6%)	228.62	5.42	0.3218	From H-1 to LUMO (90%), from HOMO to L+2 (6%)
	4	189.63	6.54	0.3266		189.95	6.53	0.3254	
	5	187.31	6.62	0.6418	From HOMO to L+2 (89%), from H-1 to LUMO (5%), from H-1 to L+9 (2%)	187.60	6.61	0.6546	From HOMO to L+2 (88%), from H-1 to LUMO (6%)
	6	180.77	6.86	0.0000		182.52	6.79	0.0000	
	7	177.99	6.97	0.0053		179.82	6.90	0.0049	
	8	175.83	7.05	0.0000		176.74	7.02	0.0000	
MeOH	1	246.76	5.02	0.0367		246.61	5.03	0.0359	
	2	230.31	5.38	0.0000		230.88	5.37	0.0000	
	3	228.19	5.43	0.3207	From H-1 to LUMO (90%), from HOMO to L+2 (6%)	228.17	5.43	0.3172	From H-1 to LUMO (89%), from HOMO to L+2 (7%)
	4	189.55	6.54	0.3303		189.86	6.53	0.3290	
	5	187.28	6.62	0.6451	From HOMO to L+2 (88%), from H-1 to LUMO (6%), from H-1 to L+9 (2%)	187.57	6.61	0.6578	From HOMO to L+2 (88%), from H-1 to LUMO (6%)
	6	180.90	6.85	0.0001		182.62	6.79	0.0001	
	7	178.14	6.96	0.0053		179.95	6.89	0.0049	
	8	175.52	7.06	0.0000		176.43	7.03	0.0000	
EtOH	1	246.45	5.03	0.0373		246.31	5.03	0.0365	
	2	231.44	5.36	0.0000		232.03	5.34	0.0000	
	3	227.97	5.44	0.3234	From H-1 to LUMO (89%), from HOMO to LUMO (2%), from HOMO to L+2 (6%)	227.97	5.44	0.3202	From H-1 to LUMO (89%), from HOMO to LUMO (2%), from HOMO to L+3 (7%)
	4	189.82	6.53	0.3426		190.13	6.52	0.3414	
	5	187.61	6.61	0.6539	From HOMO to L+2 (88%), from H-1 to LUMO (6%), from H-1 to L+10 (2%)	187.91	6.60	0.6669	From HOMO to L+3 (87%), from H-1 to LUMO (6%)
	6	181.24	6.84	0.0001		182.96	6.78	0.0001	
	7	178.58	6.94	0.0051		180.39	6.87	0.0048	
	8	175.23	7.08	0.0000		176.16	7.04	0.0000	

Note: H and L represents the molecular orbital of the HOMO (H) and LUMO (L), respectively.

3.3. AIM analysis

Topological geometry of a benzoic acid dimer using AIM software is shown in Fig. 3. Topological parameters for the title compound dimer are given in Table 4.

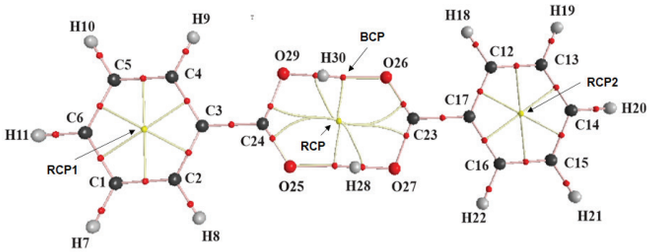

Fig. 3. Topological geometry of BCP (small red spheres) and RCP (small yellow spheres) for a benzoic acid dimer calculated with B3LYP/6-311++G(2d,p).

From Table 4, the electron density (ρ(rc)) and Laplacian ($\nabla^2\rho(rc)$) at the BCP of H···O contacts are 0.051 and 0.126 a.u., respectively. They all fit within the criteria for formation of hydrogen bonds (HBs) [21]. The O–H···O interactions are partly covalent in nature as indicated by $\nabla^2\rho(rc)>0$ (0.126 a.u), $H(rc)\leq 0$ (-0.007), and $G/|V(rc)|\leq 1$ (-0.846 a.u). The strength of the hydrogen bond interaction increases with increasing local electron density at BCP of HBs through the hydrogen bond energies (E_{HB}). In this work, E_{HB} was calculated to be -59.6 kJ.mol^{-1}. The calculated value of E_{HB} affirmed that the HBs found in the title compound belong to strong hydrogen bonding [3, 22].

Table 4. AIM analysis for a cyclic dimer of benzoic acid using B3LYP/6-311++G(2d,p).

Parameter	O–H	O–H···O	RCP1[a]	RCP2[b]	RCP[c]
ρ(rc)	0.321	0.051	0.023	0.023	0.009
$\Delta^2\rho(rc)$	-2.377	0.126	0.159	0.159	0.035
λ_1	-1.647	-0.093	-0.018	-0.018	-0.008
λ_2	-1.629	-0.092	0.088	0.088	0.014
λ_3	0.899	0.310	0.089	0.089	0.029
G(rc)	0.067	0.038	0.034	0.034	0.008
V(rc)	-0.728	-0.045	-0.028	-0.028	-0.007
G/|V(rc)|	-0.092	-0.846	-1.217	-1.217	-1.174
H(rc)	-0.661	-0.007	0.006	0.006	0.001

Note: [a, b, c]: labelled in Fig. 3.

3.4. Vibrational analysis

The title compound consists of 15 atoms and therefore exhibits 39 normal modes of vibrations. The monomer structure has C_1 point group symmetry. The vibrational analysis of benzoic acid is performed on the basis of the characteristic vibrations of C–H, O–H, C=O, –COOH, and phenyl ring modes. The calculated and experimental IR spectra of the title molecule are given in Fig. 4. The vibrational analysis of the title compound was performed on the basis of the characteristic vibrations of the most important excited states in the molecule. The vibrational assignments for different functional groups are discussed below.

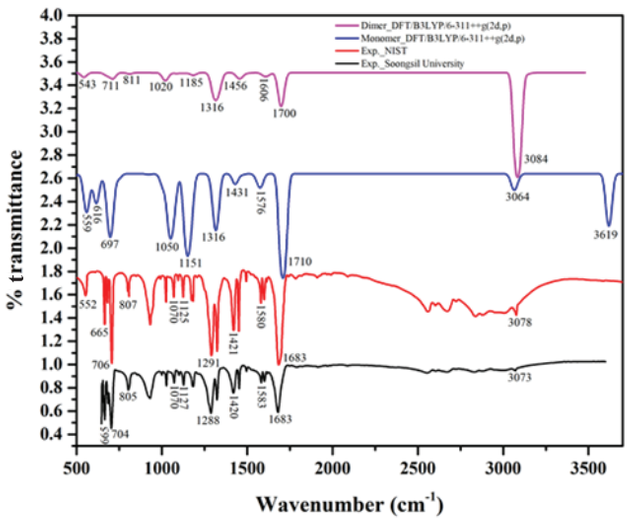

Fig. 4. Experimental and calculated FT-IR spectra of benzoic acid monomer and dimer.

Carboxylic acids group vibrations: Carbonyl and hydroxyl groups are best characterized by carboxylic acid groups. When a non-hydrogen bond is observed in the region 3700-3500 cm^{-1}, the existence of a hydrogen bond formation lowers the O–H stretching frequency in the 3500-3200 cm^{-1} region. In our theoretical calculations of a

Table 5. Experimental and calculated vibrational frequencies and assignments based on potential energy distribution (PED) calculation of the benzoic acid monomer and dimer with B3LYP/6-311++G(2d,p).

No.	Frequencies (cm^{-1})			[b]Assignments based on PED calculations
	Exp.[a]	*Cal_monomer*	*Cal_dimer*	
1	552	559	543	$\delta(H_{15}\text{-}O_{14}\text{-}C_{12}\text{-}C_3)$
2	665	616	-	$\beta(O_{13}\text{-}C_{12}\text{-}O_{14}) + \beta(C_1\text{-}C_6\text{-}C_5)$
3	706	697	711	$\delta(H_7\text{-}C_1\text{-}C_6\text{-}C_5) + \delta(H_{10}\text{-}C_5\text{-}C_6\text{-}C_1) + \delta(C_3\text{-}C_2\text{-}C_6\text{-}C_1) + \gamma(O_{13}\text{-}C_3\text{-}O_{14}\text{-}C_{12})$
4	1070	1050	1020	$\nu(C_2\text{-}C_1) + \nu(O_{14}\text{-}C_{12}) + \beta(H_9\text{-}C_4\text{-}C_5)$
5	1125	1151	1185	$\beta(H_{15}\text{-}O_{14}\text{-}C_{12}) + \beta(H_9\text{-}C_4\text{-}C_5)$
6	1291	1316	1316	$\nu(O_{14}\text{-}C_{12}) + \nu(C_{12}\text{-}C_3) + \beta(H_{15}\text{-}O_{14}\text{-}C_{12}) + \beta(O_{13}\text{-}C_{12}\text{-}O_{14})$
7	1421	1431	1456	$\beta(H_7\text{-}C_1\text{-}C_2) + \beta(H_{10}\text{-}C_5\text{-}C_6) + \beta(H_{11}\text{-}C_6\text{-}C_1)$
8	1580	1576	1606	$\nu(C_2\text{-}C_1) + \nu(C_4\text{-}C_5)$
9	1683	1710	1700	$\nu(O_{13}\text{-}C_{12})$
10	-	3064	-	$\nu(C_1\text{-}H_7) + \nu(C_5\text{-}H_{10}) + \nu(C_6\text{-}H_{11})$
11	3078	3619	3084	$\nu(O_{14}\text{-}H_{15})$

Note: [a]: Frequencies_Exp.: https://webbook.nist.gov/cgi/cbook.cgi?ID=C65850&Type=IR-SPEC&Index=4; [b]: Abbreviations: ν, β, δ, and γ denote stretching, in-plane bending and torsion modes, respectively. The assignments of the vibrational frequencies were performed by PED analysis by using VEDA4 program [23].

benzoic acid monomer, the IR band at 3619 cm^{-1} is assigned to O–H stretching modes as observed in Table 5. The values of these modes show agreement with experimental values. While in the dimer, these modes are seen at 3084 cm^{-1} because the O–H stretching wave number is shifted due to resonance in the dimer. These results agree with data from literature [24]. The in-plane O–H bend and out-of-plane O–H bend vibrations occur at 1350±50 cm^{-1} and 650±50 cm^{-1}, respectively. Accordingly, an O–H out-of-plane bend can be observed in FT-IR at 559 and 543 cm^{-1} (monomer and dimer, respectively). Besides, the C=O stretching of carboxylic acids located in the region 1760-1690 cm^{-1} [25]. The biggest C=O stretching vibration in the carboxylic acid group of a benzoic acid monomer is calculated at 1710 cm^{-1}. In dimer form, these stretching modes are assigned at 1700 cm^{-1} as in Table 5.

Carbon-hydrogen vibrations: For all aromatic and heteroaromatic organic compounds, 2C–H stretching vibrations are observed in the region 3250-2950 cm^{-1} whereas the region 3250-3100 cm^{-1} contains the asymmetric stretching mode and 3100-2950 cm^{-1} contains the symmetric stretching mode of vibrations [26]. C–H bending vibrations are observed in the 1300-1000 cm^{-1} region while the out-of-plane bending vibrations occur in the 1000-675 cm^{-1} [24]. From Table 5, the C–H stretching modes of the title compound are observed in FT-IR at 3064 cm^{-1}. The calculated C–H out-of-plane bending is assigned to the bands at 697 cm^{-1}. These results are also seen in the literature [8, 27].

Carbon-carbon ring vibrations: C–C stretching vibrations usually occur within the range of 1625-1430 cm^{-1} in the ring [28]. For example, C–C stretching was observed at 1586, 1547, 1420, and 1306 cm^{-1} [29] and also at the frequencies 1369, 1551, 1584, and 1612 cm^{-1} [30]. In this study, the C–C modes for the benzoic acid monomer and dimer were observed at 1576 and 1606 cm^{-1}, respectively, and assigned by PED.

3.5. NBO analysis

NBO analysis for the benzoic acid dimer were performed using B3LYP/6-311++G(2d,p). The energy difference between donor and acceptor i and j NBO orbitals in a.u., F(i,j), which is the Fock matrix element, and $E^{(2)}$, the energy of hyper-conjugative interactions (kcal.mol^{-1}), are gathered in Table 6.

Table 6. Second order perturbation theory of the Fock matrix of a benzoic acid dimer by NBO analysis.

Interaction (donor → acceptor)[a]		E(i)–E(j)	F(i,j)	$E^{(2)b}$
LP(2) O25	σ^*C24–O29	3.17	0.308	36.12
LP(2) O29	σ^*C24–O25	3.55	0.178	10.77
LP(2) O26	σ^*C23–O27	4.13	1.109	59.30
LP(1) O25	σ^*C3–C24	7.76	9.919	87.78
LP(2) O26	σ^*C17–C23	4.13	1.109	59.30
LP(2) O25	σ^*O27–H28	4.37	0.169	7.91
LP(1) O26	σ^*O29–H30	1.88	0.232	35.36

Note: [a]: See Fig. 1 for atom numbering; [b]: kcal.mol^{-1} is the unit of $E^{(2)}$.

The O–H···O bond in the title compound dimer is confirmed by lone-pair orbital in the electron donation to the σ^* antibonding orbital for LP(O) → σ^*(O–H) interactions. The orbital interaction in lone-pairs of oxygen atoms LP(O25) → σ^*(O27–H28), LP(O26) → σ^*(O29–H30) had $E^{(2)}$ values of 7.91 and 35.36 kcal.mol^{-1} respectively. These $E^{(2)}$ values show the formation of intermolecular HBs. The existence of interactions in the dimer of benzoic acid is also confirmed by AIM analysis as shown in Fig 3. Similarly, the $E^{(2)}$ value was 87.78 kcal.mol^{-1} for the interaction (O25) → σ^*(C3–C24), which is a huge value. This results in intramolecular charge transfer causing stabilization of the molecular system.

3.6. Frontier molecular orbitals and MEP

The energies of the two most important molecular orbitals in a molecule are both used to describe various chemical properties, for example, the HOMO and LUMO and the value of energy separation between the HOMO and LUMO ($\Delta E_{HOMO-LUMO}$). Several chemical parameters, such as ionization potential (I), electron affinity (A), electronic chemical potentials (μ), global hardness (η), electrophilicity (ω), electronegativity (χ), and chemical softness (S) can be evaluated from the HOMO, LUMO energy [31-33]. The calculated results are shown in Fig. 5A. The calculated values of HOMO and LUMO energy are -7.460 and -1.791 eV, respectively. The $\Delta E_{HOMO-LUMO}$ energy gap is estimated to be 5.669 eV, which clarifies the interactions of charge transfer occurring in benzoic acid. The HOMO-LUMO gap is related to chemical reactivity or kinetic stability, and since both have negative values, they decide the chemical stability of the molecule.

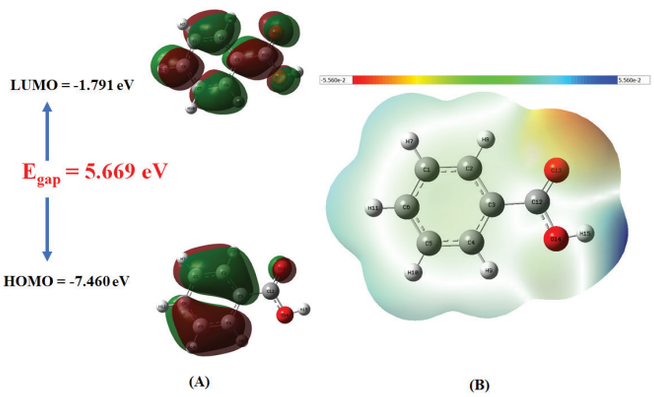

Fig. 5. (A) The frontier molecular orbitals; (B) MEP map for benzoic acid calculated by DFT at the B3LYP/6-311++G(2d,p) level.

The MEP is a plot of electrostatic potential mapped onto a constant electron density surface. The surfaces of the molecule having different electrostatic potentials are represented by various colours. The surface is coloured according to the local electrostatic potential (e.g., red/negative, green/near zero, and blue/positive). The values of the electrostatic potential decrease in the order blue > green > yellow > orange > red [34]. From the MEP shown in Fig. 5B, it is evident that the negative (red colour) charge covers the carbonyl oxygen atom O25(26) and the positive region (blue colour) covers the carboxylic acid hydrogen atom H28(30)–O25(26). This confirms the existence of an intermolecular O27(29)–H28(30)···O25(26) interaction.

4. Conclusions

In the present theoretical study, structural, vibrational, and electronic investigations with AIM, FT-IR, MEP, HOMO-LUMO, and NBO analysis of the monomer and dimer of benzoic acid have been carried with the B3LYP/6-311++G(2d,p) basis set. The geometrical parameters of bond lengths and angles have been calculated and compared with their experimental values. The solvent effect on the electronic absorption spectra of benzoic acid was analysed in the gas phase as well as in various solvents by using UV-Vis spectroscopy and DFT calculations. The HOMO-LUMO energy gap was calculated to be 5.669 eV. The low HOMO-LUMO band gap indicated that benzoic acid is more reactive and has less kinetic stability. The hydrogen bond interaction was studied by AIM analysis. The strength of the interaction was evaluated using NBO analysis through the energy of the hyperconjugative interaction $E^{(2)}$ value. The energy value of the LP(1) O26 → σ^*O29–H30 interaction was 35.36 kcal.mol^{-1} indicating the existence of hydrogen bond interactions in the dimer. The electrostatic potential map was also discussed.

CRediT author statement

Tan Trung Truong: Method, Data analysis, Writing, Edited and Revised; Phuong Dong Nguyen: Method, Data analysis, Writing; Thi Ngan Nguyen: Method, Data analysis, Writing; Thi Thu Thuy Le: Method, Data analysis, Writing; Ngoc Huong Nguyen: Method, Data analysis, Writing.

ACKNOWLEDGEMENTS

We are thankful to Professor Renjith Thomas, Changanassery 686101, Kerala INDIA and also thankful to Ph.D. Phan Dang Cam Tu, Laboratory of Computational Chemistry and Modelling, Quy Nhon University for all kind of supporting the Gaussian 09 program.

COMPETING INTERESTS

The authors declare that there is no conflict of interest regarding the publication of this article.

REFERENCES

[1] W.D. McBride, C. Greene, L. Foreman, M. Ali (2015), "The profit potential of certified organic field crop production", *USDA, Economic Research Service*, Economic Research Report no. ER-188, 52pp.

[2] N. Akhtar, A. Verma, K. Pathak (2015), "Topical delivery of drugs for the effective treatment of fungal infections of skin", *Current Pharmaceutical Design*, **21(20)**, pp.2892-2913.

[3] G.R. Desiraju, T. Steiner (2001), *The Weak Hydrogen Bond: In Structural Chemistry And Biology*, Oxford University Press, DOI: 10.1093/acprof:oso/9780198509707.001.0001.

[4] C.C. Wilson, N. Shankland, A.J. Florence (1996), "A single-crystal neutron diffraction study of the temperature dependence of hydrogen-atom disorder in benzoic acid dimers", *Journal of The Chemical Society, Faraday Transactions*, **92(24)**, pp.5051-5057.

[5] G.M. Florio, E.L. Sibert, T.S. Zwier (2001), "Fluorescence-dip IR spectra of jet-cooled benzoic acid dimer in its ground and first excited singlet states", *Faraday Discussions*, **118**, pp.315-330.

[6] G.M. Florio, T.S. Zwier, E.M. Myshakin, et al. (2003), "Theoretical modelling of the OH stretch infrared spectrum of carboxylic acid dimers based on first-principles anharmonic couplings", *The Journal of Chemical Physics*, **118(4)**, pp.1735-1746.

[7] H.T. Flakus, M. Chełmecki (2002), "Infrared spectra of the hydrogen bond in benzoic acid crystals: Temperature and polarization effects", *Spectrochimica Acta Part A: Molecular and Biomolecular Spectroscopy*, **58(1)**, pp.179-196.

[8] M. Boczar, K. Szczeponek, M.J. Wójcik, C. Paluszkiewicz (2004), "Theoretical modeling of infrared spectra of benzoic acid and its deuterated derivative", *Journal of Molecular Structure*, **700(1-3)**, pp.39-48.

[9] A. Kumer, N. Sarker, S. Paul (2019), "The theoretical investigation of HOMO, LUMO, thermophysical properties and QSAR study of some aromatic carboxylic acids using HyperChem programming", *International Journal of Chemistry and Technology*, **3(1)**, pp.26-37.

[10] A.D. Becke (1988), "Density-functional exchange-energy approximation with correct asymptotic behavior", *Physical Review A*, **38(6)**, DOI: 10.1103/PhysRevA.38.3098.

[11] C. Lee, W. Yang, R.G. Parr (1988), "Development of the Colle-Salvetti correlation-energy formula into a functional of the electron density", *Physical Review B*, **37(2)**, DOI: 10.1103/PhysRevB.37.785.

[12] R.A. Kendall, T.H Dunning, R.J. Harrison (1992), "Electron affinities of the first-row atoms revisited. Systematic basis sets and wave functions", *The Journal of Chemical Physics*, **96(9)**, pp.6796-6806.

[13] F. Biegler-König, J. Schönbohm (2000), *AIM 2000 1.0*, University of Applied Sciences: Bielefeld, Germany.

[14] E. Glendening, J.K. Badenhoop, A.E. Reed, et al. (2001), *Gen NBO 5.G*, Theoretical Chemistry Institute: University of Wisconsin.

[15] P. Politzer, P.R. Laurence, K. Jayasuriya (1985), "Molecular electrostatic potentials: an effective tool for the elucidation of biochemical phenomena", *Environmental Health Perspectives*, **61**, pp.191-202.

[16] M.J. Frisch, G.W. Trucks, H.B. Schlegel, et al. (2009), *Gaussian 09*, https://gaussian.com/g09citation/, accessed 20 October 2021.

[17] R. Dennington, T. Keith, J. Millam (2009), *GaussView*, Version 5, https://www.scirp.org/(S(vtj3fa45qm1ean45vvffcz55))/reference/ReferencesPapers.aspx?ReferenceID=1958990, accessed 20 October 2021.

[18] G.A. Sim, J.M. Robertson, T.H. Goodwin (1955), "The crystal and molecular structure of benzoic acid", *Acta Crystallographica*, **8(3)**, pp.157-164.

[19] C.C. Wilson, N. Shankland, A.J. Florence (1996), "Direct determination of the temperature dependence of proton transfer in the benzoic acid dimer by single crystal neutron diffraction", *Chemical Physics Letters*, **253(1-2)**, pp.103-107.

[20] T. Yanai, D.P Tew, N.C. Handy (2004), "A new hybrid exchange-correlation functional using the Coulomb-attenuating method (CAM-B3LYP)", *Chemical Physics Letters*, **393(1-3)**, pp.51-57.

[21] U. Koch, P.L. Popelier (1995), "Characterization of CHO hydrogen bonds on the basis of the charge density", *The Journal of Physical Chemistry*, **99(24)**, pp.9747-9754.

[22] G.A. Jeffrey (1997), *An Introduction to Hydrogen Bonding*, Oxford University Press, 320pp.

[23] M.H. Jamroz (2004), "Vibrational energy distribution analysis VEDA 4", *Warsaw Business Journal*, https://www.scienceopen.com/document?vid=c3aca357-33d7-4fa8-8fb3-6711575c8e32, accessed 20 October 2021.

[24] N. Issaoui, H. Ghalla, S. Muthu, et al. (2015), "Molecular structure, vibrational spectra, AIM, HOMO-LUMO, NBO, UV, first order hyperpolarizability, analysis of 3-thiophenecarboxylic acid monomer and dimer by Hartree-Fock and density functional theory", *Spectrochimica Acta Part A: Molecular and Biomolecular Spectroscopy*, **136**, pp.1227-1242.

[25] M. Kędzierska-Matysek, A. Matwijczuk, M. Florek, et al. (2018), "Application of FTIR spectroscopy for analysis of the quality of honey", *BIO Web of Conferences*, **10**, DOI: 10.1051/bioconf/20181002008.

[26] R.M. Silverstein, G.C. Bassler (1962), "Spectrometric identification of organic compounds", *Journal of Chemical Education*, **39(11)**, DOI: 10.1021/ed039p546.

[27] S.G. Stepanian, I.D. Reva, E.D. Radchenko, G.G. Sheina (1996), "Infrared spectra of benzoic acid monomers and dimers in argon matrix", *Vibrational Spectroscopy*, **11(2)**, pp.123-133.

[28] E.B. Sas, M. Kurt, M. Can, et al. (2016), "Spectroscopic studies on 9H-carbazole-9-(4-phenyl) boronic acid pinacol ester by DFT method", *Journal of Molecular Structure*, **1118**, pp.124-138.

[29] V. Dixit, R.A. Yadav (2015), "Experimental IR and Raman spectroscopy and DFT methods based material characterization and data analysis of 2-Nitrophenol", *Biochemistry and Pharmacology*, **4**, DOI: 10.4173/2167-0501.1000183.

[30] E.G. Lewars (2003), *Computational Chemistry*, Springer Dordrecht, DOI: 10.1007/978-90-481-3862-3.

[31] K. Fukui (1982), "Role of frontier orbitals in chemical reactions", *Science*, **218(4574)**, pp.747-754, pp.747-754.

[32] E.A.M. Gad, E.M.S. Azzam, S.A.H. Hussien (2018), "Theoretical approach for the performance of 4-mercapto-1-alkylpyridin-1-ium bromide as corrosion inhibitors using DFT", *Egyptian Journal of Petroleum*, **27(4)**, pp. 695-699.

[33] M. Miar, A. Shiroudi, K. Pourshamsian, et al. (2020), "Theoretical investigations on the HOMO-LUMO gap and global reactivity descriptor studies, natural bond orbital, and nucleus-independent chemical shifts analyses of 3-phenylbenzo [d] thiazole-2 (3 H)-imine and its para-substituted derivatives: Solvent and substituent effects", *Journal of Chemical Research*, **45(1-2)**, pp.147-158 DOI: 10.1177/1747519820932091.

[34] I. Warad, O. Ali, A.A. Ali, et al. (2020), "Synthesis and spectral Identification of three Schiff bases with a 2-(piperazin-1-yl)-N-(thiophen-2-yl methylene) ethanamine moiety acting as novel pancreatic lipase inhibitors: Thermal, DFT, antioxidant, antibacterial, and molecular docking investigations", *Molecules*, **25(9)**, DOI: 10.3390/molecules25092253.